METHODS OF NATURAL SCIENCES IN THE STUDY OF CULTURAL HERITAGE OBJECTS

On the Mystery of One Bead

E. Yu. Tereschenko[a,b,c,*], I. N. Kuzina[d,], A. V. Mandrykina[a,b], O. A. Kondratev[a], E. S. Kulikova[a],
R. D. Svetogorov[a], P. V. Gureva[a], E. S. Kovalenko[a], M. M. Murashev[a], E. S. Vaschenkova[a,b],
A. M. Ismagulov[a,b], V. M. Retivov[a,b], and E. B. Yatsishina[a,b]**

[a] National Research Center "Kurchatov Institute," Moscow, Russia
[b] National Research Center "Kurchatov Institute"—IREA, Moscow, Russia
*[c] Shubnikov Institute of Crystallography, Federal Research Center Crystallography and Photonics,
Russian Academy of Sciences, Moscow, Russia*
[d] Institute of Archeology, Russian Academy of Sciences, Moscow, Russia
***e-mail: elenatereschenko@yandex.ru**
****e-mail: kuzina.i65@mail.ru**
Received May 4, 2022; revised July 15, 2022; accepted July 18, 2022

Abstract—The results of studying a biconical glass bead (14th century) found during excavations by the Institute of Archaeology, Russian Academy of Sciences, at the settlement of Rostislavl (urban district of Kolomna, Moscow oblast) in 2018 are presented. The studied bead specimen differs significantly from all beads traditionally found during excavations in this region. A combination of a complex of imaging methods (X-ray and neutron tomography), large-scale X-ray fluorescence mapping of the distribution of elements, scanning electron microscopy with energy-dispersive X-ray microanalysis, and phase analysis allow us to determine that the bead decoration was formed by several layers of materials of different composition. Quantitative information about the base composition and trace components is obtained by laser ablation inductively coupled plasma mass spectrometry. It is revealed that the bead was made by combining separate layers of the base and decorating material from glasses of two classes, lead silicate and potash lead. Both established glass classes bring it closer to the medieval glasses of Central Europe. In this case, such a combination of the composition and manufacturing technique of similar objects was first found on the territory of Old Russia.

INTRODUCTION

The use of methods of natural sciences in the study of cultural heritage objects is becoming more widespread. The combination of a wide range of modern methods of materials science and humanitarian research on material traces of human activity in this interdisciplinary field creates an opportunity for significant expansion of the information potential of historical materials. One of the striking examples of successful cooperation in the field of historical materials science was a series of joint studies of various archaeological finds conducted by specialists from the National Research Center "Kurchatov Institute" and the Institute of Archaeology, Russian Academy of Sciences. A series of works on the study of medieval blackened encolpion crosses [1–9] and other pieces of personal piety, in particular, an enamel icon [10] and a gold quadrifoil with an enamel insert [11], an antique ceramic head [12–14], found in Kerch during the construction of the Crimean bridge, as well as other objects [15], allowed us to obtain more extensive information about the development of technologies, cultural and trade relations of regions and communities in different historical periods.

This paper presents the study of a glass bead, a unique find excavated by the Rostislavl archaeological expedition of the Institute of Archaeology, Russian Academy of Sciences, in 2018 at the Rostislavl settlement in the urban district of Kolomna, Moscow oblast, tentatively dated to the first half of the 14th century.

The aim of the work was to study the composition, structure and structural features of the bead to clarify its origin, which determined the complex nature of the studies performed.

THE OBJECT OF THE STUDY AND HISTORICAL CONTEXT OF THE FIND

The archaeological site, Rostislavl Settlement, is located on the middle Oka, not far from the confluence of the Osetr River [16]. This archaeological site corresponds to the Old Russian city of Rostislavl, founded, according to the chronicles, in 1153 by an opponent of Yurii Dolgorukii, knyaz Rostislav Yaro-

slavich from the Chernigov branch of the Rurikovich. To distinguish from other cities with the same name in publications, the city is called Rostislavl Ryazanskii. It belongs to the so-called small towns of Old Russia ([17], p. 100).

The history of the city is little known, although from time to time it appeared on the pages of written sources. The city recovered after the Batu invasion and even became a princely residence for some period, but after flourishing in the first half of the 14th century very soon, for various reasons, life in it became less and less active, and by the 17th century, Rostislavl lost the status of a city.

Rostislavl Ryazanskii had defensive fortifications, fixed today along a rampart with a moat. The fortified city center was located on a high promontory formed by a deep ravine. There was an urban settlement and unfortified rural settlements around. The area of the fortified part of the city was 2.5 ha.

Archaeological studies showed that settlements on the site of the future city existed long before its appearance. The site contains cultural strata of the early Iron Age, Bronze Age, and Stone Age. In the 20th century, the territory of the archaeological site was actively plowed and used for various economic purposes. In 1995, the settlement of Rostislavl Ryazanskii was recognized as a site of federal significance. Excavations have been carried out here continuously since 1994 under the supervision of V.Yu. Koval'.

The object of the study refers to the material culture of the population of the 14th century. Despite the success of intensive archaeological research in recent decades, many features of the material culture of that time still remain unclear. Glass jewelry, bracelets and beads, practically disappears from the everyday life of the population of Old Russia with the disappearance of their own glass making craft and a change in trade relations. The finds known to archaeologists belong mainly to the production of the Golden Horde. In Rostislavl itself in the complexes of the 14th century glass beads are rare.

The studied bead (the passport of the find: excavation II, site ЬI, pit 797, square 276, depth −241, no. 62 according to the field inventory) is dated by the supervisor of the excavations according to stratigraphic materials. It was found (Fig. 1a) at the bottom of pit 797, at an excavation within the boundaries of the fortified part of the medieval city ([18], pp. 34−38). The pit, 65 cm deep, had a subrectangular shape, elongated along the north−north-west−south−south-east line (dimensions 280 × 200 cm), almost sheer walls, rather sharply turning into a flattened bottom that slightly bended towards the center. In the eastern part of the bottom, there were four unequal depressions (depth from 4 to 55 cm). The filling of the pit was uniform and consisted of yellow loam with inclusions of dark gray loam, coals, and pieces of stove; four rounded depressions at the bottom of the pit were filled with a mixture of yellow and gray loam.

Together with the bead, nine more individual finds were found in pit 797: two intact iron knives and a fragment of a nonferrous metal a pectoral cross, and four ceramic pots in pieces. To these, objects from the upper part of the eastern half of the pit should be added: an iron knife, a signet ring made of lead-tin alloy with the image of a human hand on a shield, and a horn spindle whorl ([18], Figs. 210−214, Tables 5−9).

Among the finds listed, there are obvious pre-Mongolian objects, for example, a cross worn next to the skin made of copper alloy with enamel decoration, yellow on one side and green on the other. All of these objects were relocated to the pit with a backfill layer. For dating of the pit, the ceramic material, the broken pieces of pots collected in different parts of the pit, mainly in the upper part of its filling, is of the greatest importance. According to the reconstructed form and wavy decoration, they belong to the Golden Horde era and individually can be dated fairly widely. However, among them there are no vessels that have transitional features from pre-Mongolian ceramics to later ones; therefore, in a single set, formed over a short period of time, they must be attributed to the second half of the 14th century.

The mass material from the described objects is also dated to the Golden Horde era: about 400 fragments of ceramics of a relatively early stage, i.e., the first half to the middle of the 14th century.

The ceramic set of another pit, 795, which cut through pit 797, belongs to the second half of the 14th century. Since the broken pieces of pots from pit 797 date back to the same time, despite the earlier mass material, according to Koval', it was dug out around the middle of the 14th century, and back filled during the middle−second half of the 14th century by native soil with inclusions of the cultural layer surrounding it.

The body of the bead has a rounded shape in the form of two cones combined at the base with slightly truncated tops. The name "biconical" was proposed for such beads by A.V. Artsikhovskii ([19], p. 34). Bead diameter of 19.8 mm and height of 18.8 mm. The channel is cylindrical with a hole diameter of 4.2 mm. The edge of one hole is convex and uneven, the other is hidden by a single decorative roller superimposed on top (Fig. 1b). The color of the body is dark, possibly brown, but cannot be more precisely determined due to corrosion of the material. The object is opaque.

The decoration consists of roller around one hole (yellowish, almost white, with traces of damage) and wavy lines (multiple yellow and white curved lines). Such curved lines are created by various techniques, for example, by pulling threads superimposed on the base with a spike. A similar effect is achieved by connecting separate interlayered segments of the base material (for example, [20]). In both cases, recessed stripes are left on the object, either from a tool or at the
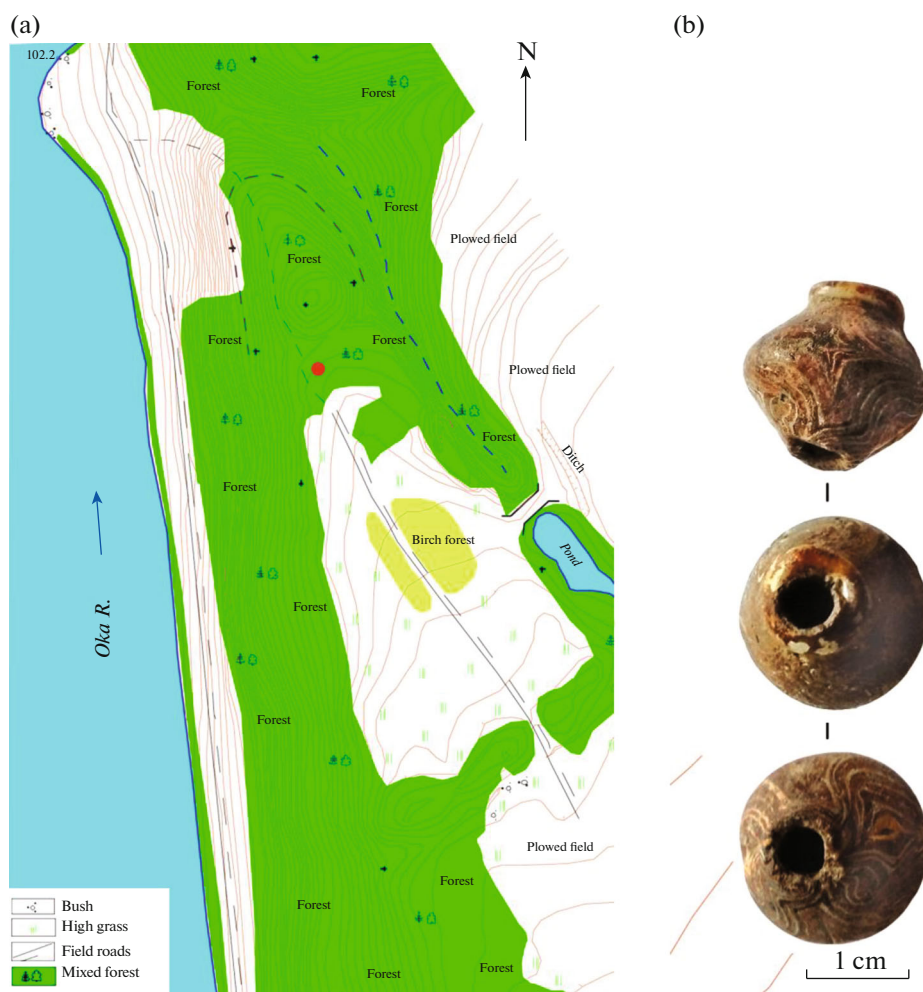
(a)　　　　　　　　　　　　　　　　　　　　(b)

Fig. 1. Topoplan of the settlement of Rostislavl, the area where the bead was found is marked with a circle (a). Drawing by Koval'. The appearance of the bead (no. 62, 2018) (b).

junctions of base segments. These traces rarely remain after additional surface treatment of the piece: rolling and fire polishing. That is why, quite often, researchers are not able to determine the decorating technique on the whole object: from layered glass or superimposed threads.

The studied piece differs significantly from all Old Russian beads currently known to us: it is unusually heavy in weight compared to its size. This feature presupposes a different composition of the base material and, perhaps, of the decoration, which is why a complex analysis of the object is necessary to discuss its complete analogues.

EXPERIMENTAL

Based on the above-described possible technological features of manufacturing the bead and identifying its material, the study should combine the analysis of the morphology, visualization of the internal structure, and determination of the elemental and phase composition. Therefore, the set of studies of the bead

included optical microscopy, X-ray and neutron tomography, X-ray fluorescence (XRF), scanning electron microscopy with energy-dispersive X-ray microanalysis (SEM/EDS), laser ablation inductively coupled plasma mass spectrometry (LA-ICP-MS), as well as synchrotron X-ray diffraction (SR-XRD) of the composition. For comparison with published data on archaeological glasses, the results of the analysis of the composition by SEM/EDS and LA-ICP-MS were recalculated into oxides ([21], pp. 14, 15, 44).

To study the bead by optical microscopy, a Stemi 2000C Zeiss microscope was used, magnification ×5 and ×20.

Studies of the internal structure were carried out using neutron and X-ray tomography. Neutron tomography of the biconical bead was carried out on a setup with a polychromatic neutron spectrum on the horizontal experimental channel 7b of the IR-8 research reactor. The spectrum maximum corresponded to a wavelength of ~1 Å. Neutron projections were recorded with a position-sensitive detector con-
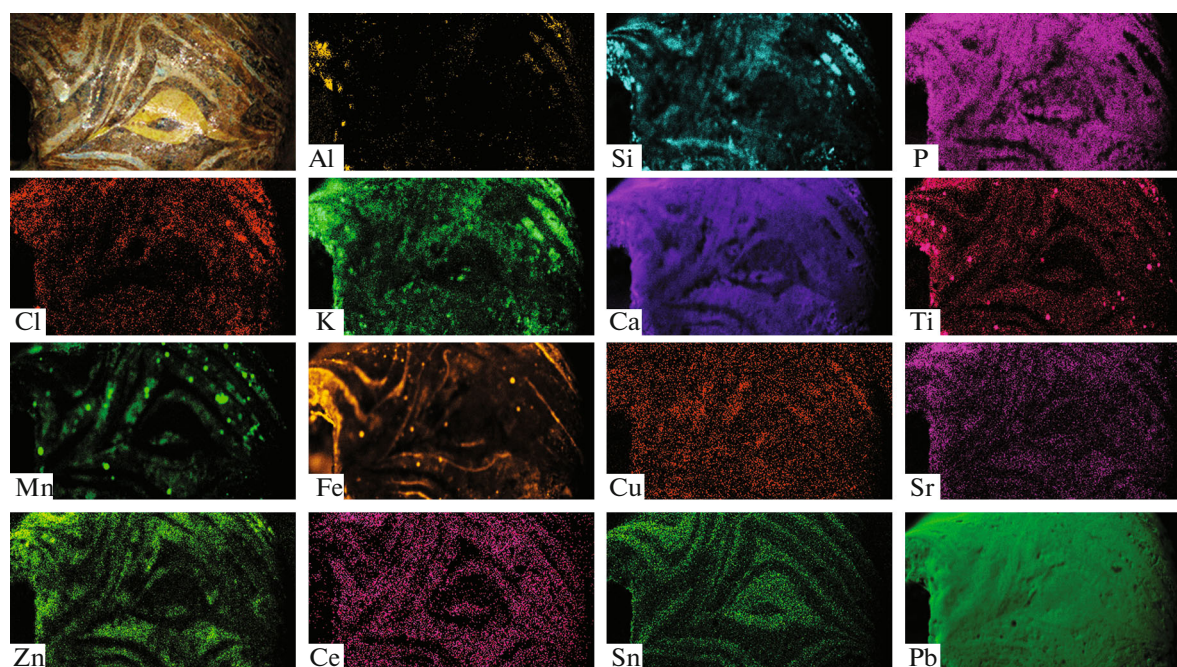
Fig. 2. Area of large-scale mapping of the distribution of elements by the XRF method and results of XRF mapping of the distribution of elements over the surface of the bead.

sisting of a scintillation screen based on a mixture of ZnS(Ag) and ^{6}LiF with a thickness of 100 μm, a mirror, an objective lens, and a CCD matrix of 2048 × 2048 pixels with a dynamic range of 16 bits. The exposure time of one frame was 350 s. The object was rotated relative to the vertical axis with a step of 0.5°. The pixel size of the obtained images was 65 × 65 μm.

X-ray tomography was performed on an X5000 (NSI) industrial X-ray tomograph in two operating modes. Shadow projections were recorded with a Perkin Elmer position-sensitive X-ray detector with a matrix size of 2048 × 2048 pixels, pixel size of 200 × 200 μm, and dynamic range of 16 bits. A direct deposition scintillator based on CsI:Tl was used. Full tomography of the bead was performed using a closed-type tube at a voltage of 450 kV and current of 1450 μA. In this case, the size of the focal spot was 400 μm. A copper filter with a thickness of 15.7 mm was used to form the spectrum of the tube. The exposure time for one frame was 1 s. The object was rotated relative to the vertical axis with a step of 0.1°. The pixel size of the images was 135 × 135 μm. Also tomography of the surface layers with a high spatial resolution was additionally performed using an open-type microfocus X-ray tube at a voltage of 100 kV and a current of 330 μA. In this case, the size of the focal spot was 33 μm. Filters were not applied. The exposure time for one frame was 1 s. The object rotated relative to the vertical axis with a step of 0.2°. The pixel size was 16 × 16 μm. Thus, the structure of the surface layers was studied to a depth of ~0.5 mm.

When processing the neutron imaging data, the ImageJ software package was used to correct images for background noise and normalize to the incident beam [22]. The tomographic reconstruction of 3D images from a set of angular projections was performed by the method of convolution and backprojection [23] using the Octopus Reconstruction 8.6 software package [24]. The reconstruction of tomographic sections and visualization of the X-ray tomography data were performed using efX-CT and Volume Graphics studio 3.5.1 software packages [25].

Large-scale X-ray fluorescence mapping of the distribution of elements over the surface of the bead (Fig. 2) was performed using an M4 Tornado microfluorescence spectrometer (Bruker): Rh anode, accelerating voltage 50 kV, current 300 μA, focusing with a polycapillary lens with a spot diameter of 25 μm. The scanning step was 50 μm. The sample chamber was evacuated (20 mbar) to record the fluorescence yield from light elements, starting with Na. The analysis of the obtained maps of the distribution of elements (without reducing the content of elements to 100%) was carried out using the M4 Tornado software.

Analysis of the base composition and trace components (SEM/EDS and LA-ICP-MS) was carried out in the region of a transverse cleavage, the surface of which was prepared by mechanical grinding (Fig. 3).

The study of the elemental composition of areas of different colors, as well as mapping of the distribution of elements by the SEM/EDS method, was performed using a Helios Nanolab 600i dual-beam scanning electron microscope with a focused ion beam

(Thermo Fisher Scientific), equipped with an EDS system, at an accelerating voltage of 30 kV in the high vacuum mode. (10^{-4} Pa). The EDS spectra and element-distribution maps were processed using the TEAM (EDS) software. The total content of the detected elements was brought to 100%. The sensitivity of the method is 0.1−0.5 wt %. SEM images were obtained using a Versa 3D dual-beam scanning electron microscope with a focused ion beam (Thermo Fisher Scientific) in the low vacuum mode (30 Pa) at an accelerating voltage of 20 kV. EDS measurements of the composition of different areas of the bead were performed at three to five points, the data of which were then averaged.

For LA-ICP-MS measurements, an ELAN DRC-e inductively coupled plasma mass spectrometer (Perkin Elmer) with an NWR 213 laser-sampling attachment (ESI New Wave Research) was used. Calibration was performed using a standard NIST SRM 610 glass sample. The laser-beam-spot diameter was 25 μm, the mass measurement time was 25 ms, and the number of replicas was 15. Three measurements were performed for each analysis area, the results of which were averaged.

The main advantage of laser sampling over the classical solution method in ICP analysis is the absence of the stage of transferring the test sample into a solution, which is very important when analyzing objects for which only nondestructive testing methods can be used. The disadvantage of this type of sampling during the study and description of the composition of macroobjects is the high locality of the method, and due to which a large heterogeneity of the object can lead to a significant error. Another disadvantage of this method is manifestation of the elemental-fractionation effect caused by different boiling points of the standard and the sample due to different composition or density, which leads to a large influence of the sample-surface morphology on the intensity of the received signals from the analytes. Taken together, these effects can cause a significant analysis error, ~10 rel. %, which is unacceptable for the analysis of macrocomponents (base composition). Partially leveling the effects caused by the different composition and state of the sample surface is possible using the method of calibration in relative concentrations followed by normalization to 100% [26]. Since the analyzed materials, both the standard and the sample, are oxide-silicate systems, in this case it will be fair to carry out normalization to 100% by oxides, and use silicon as an internal standard. One of the causes for the error in overestimating the content of components in this calculation method is the presence of volatile and undetectable substances (carbonates, hydrated water), as well as the presence of nonhigher oxides. For correction in the analysis of geological objects, the mass loss after calcination is summed to 100%. The studied object in this work is not of natural origin, and the content of hydrated water and possible carbonates is absent or
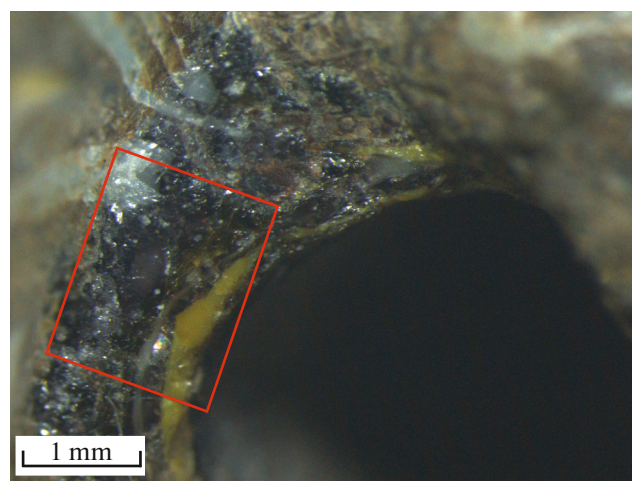

Fig. 3. Area of the bead without roller. The area used for SEM/EDS and LA-ICP-MS studies is highlighted.

insignificant in comparison with the error of the analysis performed.

The mathematical apparatus for calculating the content of elements in SEM/EDS (calculation of the oxygen content by stoichiometry and normalization to 100%) does not take into account the possible content of nonhigher oxides [27]. In this regard, in order to compare the results of different studies when analyzing by LA-ICP-MS and SEM/EDS, it would be correct to disregard the possible content of nonhigher oxides. For the studied object, it is not possible to determine the mass loss after calcination, since it is of value and only noninvasive or minimally invasive (as in the case of LA) methods are applicable in the analysis.

The SR-XRD analysis of two samples from the bead was carried out at the X-ray diffraction analysis station of the Kurchatov Specialized Source of Synchrotron Radiation KISI-Kurchatov [28]. The recording of two-dimensional diffraction patterns was carried out using a Rayonix SX165 position-sensitive detector, located at a distance of 80 mm from the sample perpendicular to the incident X-ray beam, at room temperature. The wavelength of the incident monochromatic radiation was 0.74 Å, the size of the photon beam was 400×400 μm^2, and the measurement time for one diffraction pattern was 2 min. The obtained two-dimensional patterns were reduced to the form $I(2\theta)$ standard for powder diffraction patterns due to azimuthal integration in the Dionis program [29]. The phase composition was determined using the PDF-4+ database using the corundum-number method [30].

RESULTS

Optical studies by a microscope confirmed the opacity of the material. The base of the bead is of an indefinite dark color due to a corrosion crust covering its entire surface. On the area cleaned of the crust, the

glass reflects light, i.e., the glass is not opaque, and its opacity must be explained by a large amount of dye. The colored stripes of the decoration are slightly convex, rising above the base up to 0.1 mm. All the elements are largely affected by the devitrification process: a partial loss of the surface layer is noticeable in cavities at higher magnification. The decorative molding around the hole of the channel was damaged more than other elements, but retained its shape and color due to a thin surface layer. Restorers attribute such destruction of archaeological finds to groups 2 and 3 of soil (chemical) glass corrosion ([31], pp. 21, 22). A dark coating is recorded inside the channel, which does not allow its surface to be studied. A dark coating partially covers the decorative molding and the bead itself.

Traces of technological operations are almost unreadable. In several cases, grooves and depressions are noticeable at the junctions of the decorative elements. Thus, the analysis of the morphology of the object did not clarify the manufacturing technology of the bead.

According to neutron and X-ray tomography, the object is in good condition, no cracks are observed. Neutron tomography on the surface of the bead revealed a layer of uneven thickness (does not exceed 200 μm), which, on average, attenuates neutrons by ~2.8 times more than the material of the bead (Figs. 4a, 4c, 4d, 1). It can be assumed that this is a corrosion layer, and it is observed mainly in the areas of the brown-colored surface (Fig. 4b). The object reveals multiple inclusions of various morphology and sizes evenly distributed over the volume. Plate-like inclusions up to $2.6 \times 1.2 \times 0.4$ mm in size, probably of mineral origin, predominate (Figs. 4a, 4c, 2). In X-rays, these inclusions do not contrast with respect to the material of the bead, which may indicate the presence of hydrogen-containing compounds in them. In addition to plate-like inclusions, single rounded inclusions up to 0.6 mm in diameter, which attenuate the neutron flux by ~4−6 times more than the bead substance, are observed (Figs. 4a, 4d, 3), and they are also contrasting in X-ray radiation (Fig. 5a).

According to the data of neutron and X-ray tomography, in addition to inclusions, the bead contains many rounded pores of various sizes, fairly evenly distributed over its volume. Pores with a volume of ~0.5−1 mm³ predominate. Single large pores are located in the central part of the bead; they have a volume of 3−11 mm³. Some of them closely adjoin the central channel (Fig. 4d, 4; Fig. 5b). The diameter of the channel was determined exactly as 4.22−4.25 mm.

Analysis of the pore distribution over the volume (Fig. 5) showed that pores with a volume of ~0.5−1 mm³, distributed over the periphery of the sample, predominate. Single large pores are located in the central part of the bead and are elongated around the channel; they have a volume of 3−11 mm³. Also, large pores are located in the upper and lower parts of the bead and have a volume of 0.5−3 mm³. The total pore volume was ~5.6% of the total volume of the object. The total volume of inclusions was ~0.59% of the total volume of the object, of which ~0.01% is spherical inclusions (Fig. 5a).

In the surface regions of the bead, stripes, the X-ray attenuation for which is ~15% higher than that of the base material, are observed. The stripes correspond to the white and yellow decoration on the surface of the bead (Figs. 6a, 6b). The material of some decorative stripes stands out against the background of the base over the entire thickness of the bead (Figs. 6b, 6c; the area is marked with an arrow). Thus, we can conclude that the decorative strips are not applied to the surface of the bead, but are embedded in the base material.

Based on tomographic data, the density of the bead was estimated. The weight of the bead was 9.43 g. According to the results of neutron tomography, the volume was 2.26 cm³. Thus, the density of the bead was 4.17 g/cm³. Based on the results of X-ray tomography, the volume and density of the bead were also calculated. The volume was 2.20 cm³, and the density was 4.30 g/cm³. The difference with the estimation by neutron tomography is probably due to the greater sensitivity of X-ray tomography to the determination of small pores and, consequently, to the smaller calculated volume of the sample. This density value is typical for glasses with a high lead content (for which it can reach ~6 g/cm³).

Analysis of the distribution of elements on the surface of the bead and its correlation with the figure on the surface was performed by large-scale XRF mapping (Fig. 2). The results obtained are considered qualitative, since according to the tomographic data, there is a rather thick corrosion layer (up to 200 μm) on the surface of the bead (Fig. 4). And although the depth of X-ray radiation penetration is several hundred microns, the exit depth of characteristic fluorescent radiation is much smaller, especially for light elements. Therefore, the contribution of the corrosion layer to the data on the elemental composition is very significant.

According to the element-distribution maps (Fig. 2), Pb is present in the entire bead, while Sn and K are present in the decorated areas, and white and yellow stripes barely differ in composition, except for the content of K. Since the distribution of Zn is practically inverse to the distribution of Sn, it can be concluded that Zn is contained predominantly in the base material. It should be noted that in the areas of the base adjacent to the white decor, an increased content of Fe was revealed. The distribution of Mn and Ti has a point character.

As noted in [27], it is more correct to perform quantitative analysis of the base composition and trace components on the surface cleaned of corrosion. Therefore, to measure the elemental composition by SEM/EDS and LA-ICP-MS in the area of bead integrity disruption, near the channel without the molding (lower part of the bead), the surface was chipped away
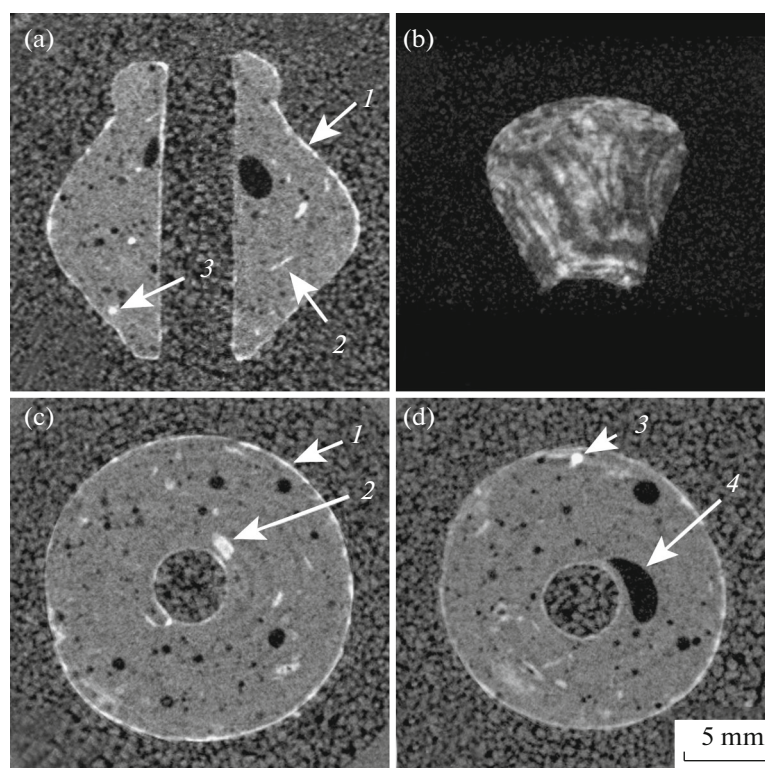
Fig. 4. Results of neutron tomography of the bead: (a) tomographic section along the channel through the geometric center of the bead; (b) fragment of the map of the neutron-attenuation maximum distribution in the surface layers of the bead; (c, d) tomographic section across the channel through the geometric center of the bead and through the large cavity 4; 1, surface layer strongly attenuating neutrons; 2, plate-like inclusions; 3, rounded inclusions; 4, large cavity adjacent to the channel wall.
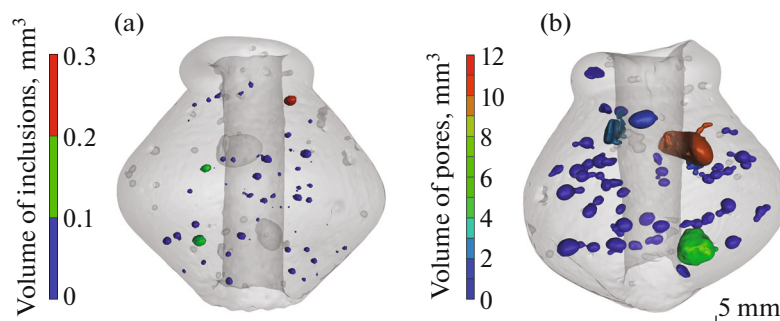

Fig. 5. Volumetric models of the distribution of inclusions (a) and pores (b) constructed based on X-ray tomography data. Pores the volume of which exceeds 1 mm^3 are shown.

and polished (Fig. 3). In the polished area, there was not only the base material, but also decorative yellow and white stripes (Fig. 7a).

According to the SEM/EDS data, the composition of the dark base is highly heterogeneous. Three main regions can be distinguished with the following compositions, for which the total content of SiO_2 and PbO_2 is about 83%, while a large scatter in the $SiO_2 : PbO_2$ ratio is observed, from 42.8 : 43.9% to 74 : 8%.

The white strip (SEM image in Table 1) showed a fairly high degree of uniformity.

A detailed analysis of the yellow decor revealed the following areas (Table 1): inclusions with a high content of Sn, the base with a high content of Pb and reduced content of Sn, and areas with a low content of Pb and Sn.

When analyzing the maps of the element distribution (Fig. 7e), inclusions were found in the areas of the base and decoration of the bead (Table 2) with increased contents of Si, Pb, and also inclusions with a very high content of Mn were found. In addition, mapping the element distribution allowed us to identify a stripe with an increased content of Fe (Table 1),
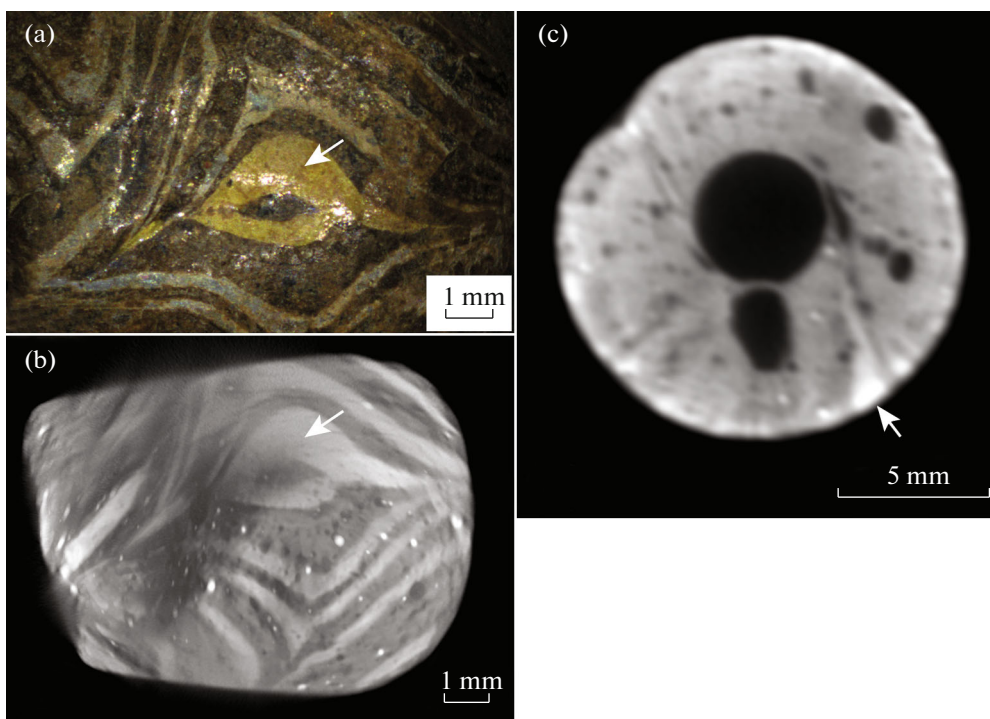
Fig. 6. Results of X-ray tomography: (a) a fragment of the surface of the bead (without the roller); (b) the distribution map of absorption maxima in the surface layer ~960 μm thick; (c) X-ray tomographic section of the bead with penetration stripes of the decoration material (marked with an arrow).

which is not distinguished by a clear boundary of a certain color in the optical image.

The analysis of trace components by LA-ICP-MS was performed in the same areas as SEM/EDS; however, the small size and rather indefinite boundaries of the white layer of the decoration did not allow us to determine its composition without including data on the base. Therefore, Tables 3 and 4 present the data on the composition of the yellow decoration and base.

We note that a high heterogeneity of the bead material, most likely due to the high degree of its destruction/corrosion, was observed.

The identification of mineral phases according to the diffraction data of two samples from different parts of the bead is given in Table 5. Amorphous phases typical for glass are not detected by XRF, and the content of the identified phases was brought to 100%.

DISCUSSION

Form and decoration, similar to the studied bead, have been known for a long time. At medieval sites of Eastern Europe, as an example, glass beads with a decoration in the form of multiple curved lines in a similar color scheme from Old Russian monuments of the 12th−13th centuries can be cited: the Mininskii archaeological complex at Lake Kubenskoe (Fig. 8, *1*, *2*), in Beloozero ([32], Figs. 152 (*3*, *12*), 153 (*5*−*7*), 171 (*2*−*5*); [33], Fig. 302 (*8*−*10*)), in burial mounds of the

Myakininskii archaeological complex near Moscow (Fig. 8, *7*).

Shchapova called such specimens beads with plastic decor ([34], pp. 88, 89, Fig. 15 (*9*, *10*)). She outlined the broad boundaries of their distribution and considered those made of "black" glass to be Russian in origin (Fig. 8, *3*).

The studied bead was found in a pit dating back to the 14th century, while objects from an earlier (pre-Mongolian) time were present with it. Therefore, this bead can be dated quite widely, given the numerous analogies in shape, decoration and color. However, it is distinguished from the pre-Mongolian beads in terms of its size: the diameter is almost 2 cm. Such beads are considered large and are found in earlier materials. Thus, specimens from the last quarter of the 1st millennium, found in Scandinavia, with a diameter of 1.8 cm or more, Kallmer classifies as macrobeads ([39], p. 35).

In Rostislavl Ryazanskii itself, according to the supervisor of the excavations, V.Yu. Koval', the cultural layer is disturbed by many years of plowing, the Old Russian layer is not distinguished stratigraphically, and, apparently, was completely absent at the location of the bead.

Among the glass beads of the Mininskii archaeological complex mentioned here (3687 pieces in total), there is not a single specimen with such dimensions, as well as among the finds in Myakinino. According to one of the authors of the article, large beads are not
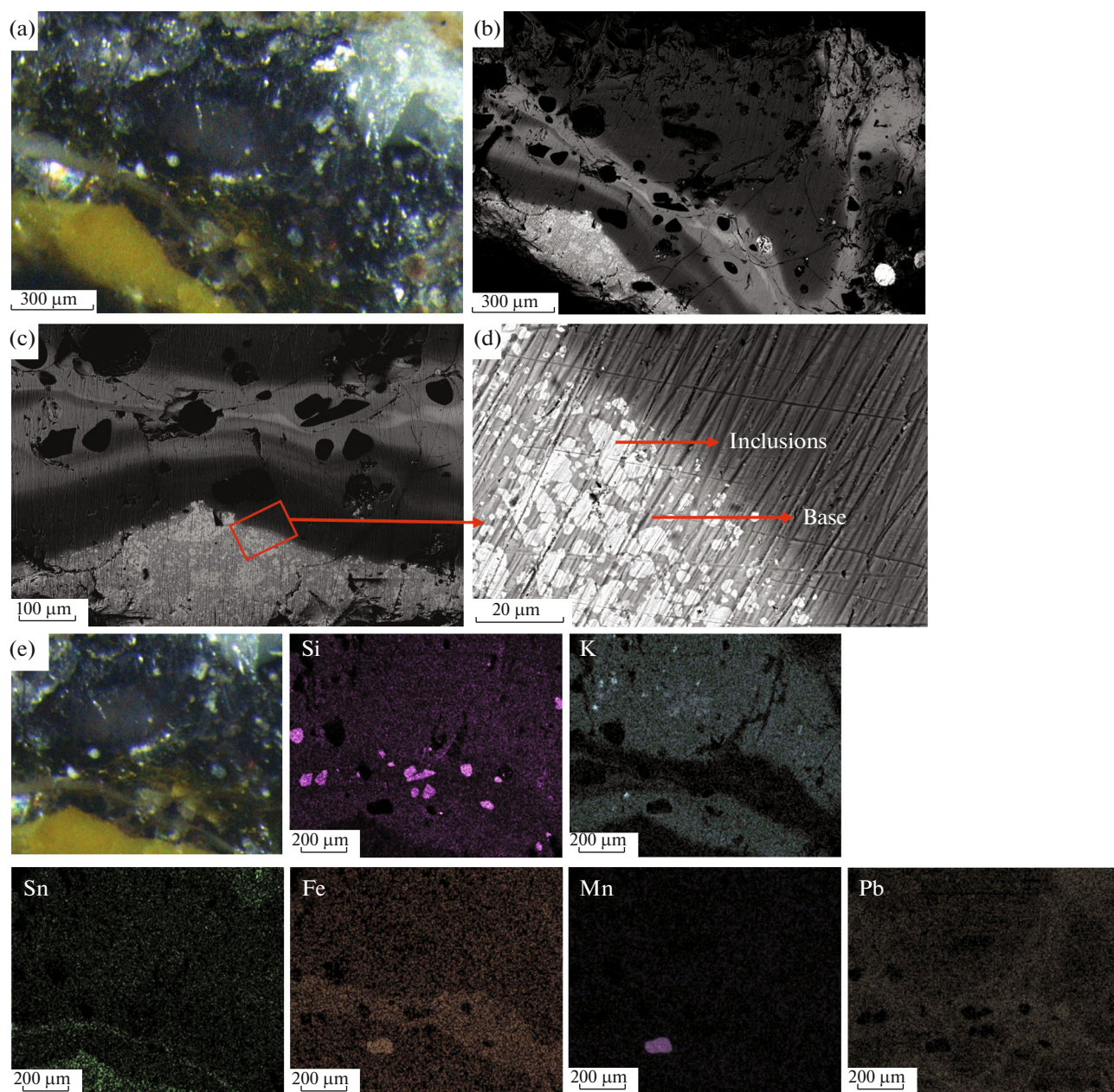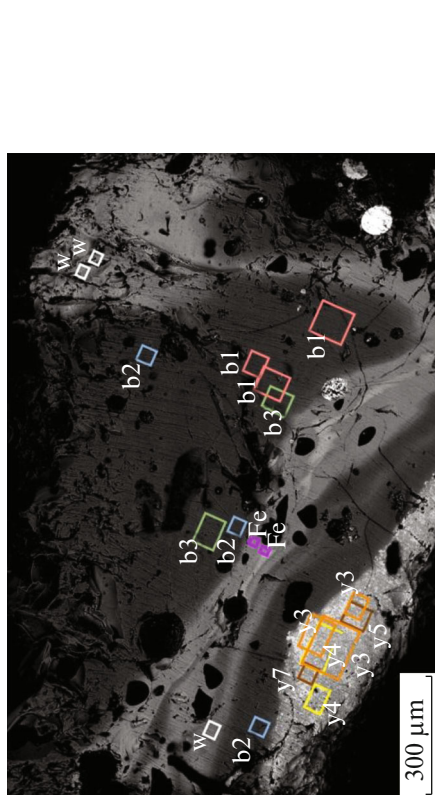
Fig. 7. Results of studies by the SEM/EDS method: (a) polished-section area; (b−d) SEM images of the polished-section area in back-scattered electrons; (e) mapping area and element distribution maps.

present in the materials of the burial grounds of Pod-bolot'evskii in Murom Poochie and Zmeiskii in the North Caucasus, corresponding in time. In the west of Eastern Europe, there is only one specimen with a diameter of 1.8 cm among more than 16 000 beads from the largest burial grounds of the Polish Pomerania of the 11th−13th centuries ([40], pp. 19, 20, 189).

In addition to the size, the studied specimen is distinguished from Old Russian beads in terms of the careful fine tuning of the shape: the vast majority of similar beads have a so-called barrel-shaped or bitrapezoid (two truncated cones, combined at the bases) shape with an indistinct edge.

Typologically, the considered specimen is closer to beads decorated with multiple curved lines from the excavations of sites of the Golden Horde period: in Ukek ([35], Fig. 1 (*25−30, 34, 37, 38*)), Bolgar ([36], p. 156, Fig. 82 (*43, 44*)), Bilyar ([37], Fig. 21 (*31, 32, 37, 38*)). In these works, such decoration is called "symmetrical strokes," "spiral-wavy," and "superimposed threads" forming "nonspiral patterns" (Fig. 8, *4−6*). It is the antiquities of the Golden Horde period at sites of the Volga region that are characterized by large beads, 20 mm and more: in Bolgar, in the Selitrennoe settlement, in Ukek and other sites; they are

Table 1. SEM/EDS data on the composition of the bead in areas of different colors (wt %)
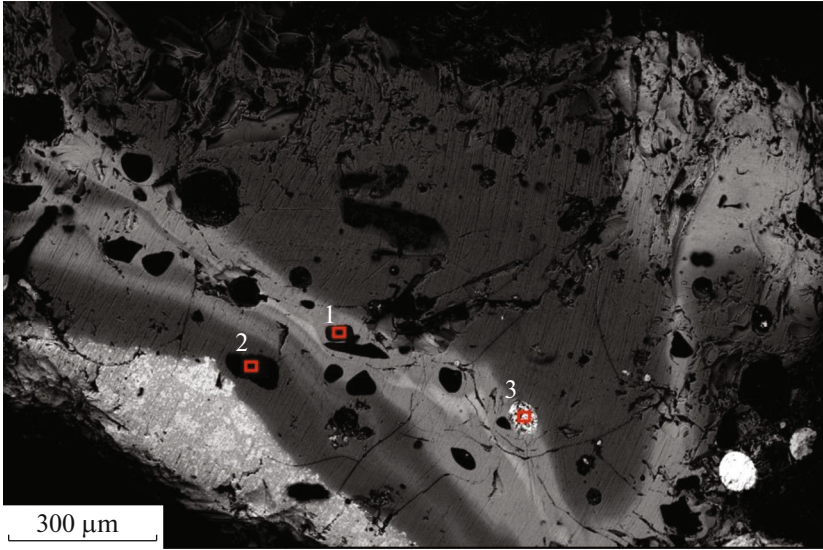
	base			white color	yellow color								band with increased iron content (Fe)
					inclusions	base	integral areas		areas distinguished by composition				
	B1	B2	B3	W	Y1	Y2	Y3	Y4	y5	y6	y7		
Na$_2$O				5.3		0.8	<0.5	<0.5		2.3	4.3		
MgO				<0.5		<0.5	<0.5						
Al$_2$O$_3$	0.9	1.1	1.1	1.5	1.4	1.4	0.9	2.7		2.0	2.9		1.0
SiO$_2$	62.6	71.6	42.9	53.1	22.1	45.4	25.8	62.4	48.1	48.3	59.0		59.6
K$_2$O	11.9	15.1	10.9		0.9	<0.5							0.8
CaO	0.9	<0.5	0.6	<0.5		1.2							
TiO$_2$	<0.5	<0.5			1.6	1.5	<0.5			3.0			
MnO	1.3	0.8	1.2										
Fe$_2$O$_3$	<0.5		<0.5	<0.5	1.3	<0.5				1.5			5.4
SnO$_2$		9.5		9.7	20.6	3.9	11.6	20.4	21.6	11.5	14.2		–
PbO$_2$	21.1	9.5	43.2	29.1	49.9	43.6	60.9	14.6	30.3	30.3	19.7		33.3

* Measurement areas Y1, Y2, and Y6 cannot be shown due to their scale incomparable with this image

Uppercase letters denote averaged data, lowercase letters denote original data. The deviation of the sum of the content of elements from 100% is caused by the presence of P, S, and Cl.

Table 2. SEM/EDS results of studying the composition of inclusions (wt %)

	Si inclusion (1)	Mn inclusion (2)	Pb inclusion (3)
Na$_2$O	0.7		
MgO			0.6
Al$_2$O$_3$	<0.5	1.3	0.8
SiO$_2$	58.9	16.1	36.2
K$_2$O		2.5	6.8
CaO			
TiO$_2$			
MnO		66.8	0.9
Fe$_2$O$_3$	1.2	3.4	<0.5
SnO$_2$			
PbO$_2$	38.9	9.8	54.1

also called pendants ([36], pp. 181−184; [41], p. 2l7; [35], pp. 260, 261).

The examples given are sufficient to conclude that the studied specimen corresponds to the antiquities of the Golden Horde period, and based on ceramic-material dating of the main filling of the pit where the bead was found, more narrowly to the 14th century.

The studies showed that the bead is made of glass with the main glass-forming elements in the form of silicon, potassium, and lead oxides, while differences in the composition of glass-forming elements are obvious in glass of different colors (Table 4).

The silicon oxide in the base of the bead is from 34.6 to 37.6%; in glass of the decoration, it is 19.4–22.9%. Lead oxide in both glasses acts as the main glass-forming agent: in the base, it ranges from 43.4–51.5%; in the yellow decoration, this indicator is higher and amounts to ~66%. The sodium content is negligible (up to 0.23%); it is present in this glass as a natural impurity or contamination. Potassium oxide is noticeable only in the base glass: here it ranges from 10.0 to 13.6%, which is sufficient for the main glass-forming component in combination with lead ([42], p. 82). The absence of calcium oxide indicates the use of potash rather than ash as the alkaline raw material. The values of aluminum oxide are also negligible (0.3–0.9%); only in two samples from the base of the bead it showed 4.0 and 8.5%: values that affected the average indicator. These cases can be considered the result of contamination or as an impurity.

The dye of the base of the bead is not obvious; this role could be played by iron oxide, but its concentration is too low (0.04–0.25%) and corresponds to an impurity to other glass components. In the absence of other obvious dyes, the glass could be dyed with carbon; for which unburned coal was introduced into the glass during melting, which inevitably led to the appearance of a noticeable amount of calcium in the glass mass, not observed in the present study ([42], pp. 31, 35). It can be assumed that the saturated dark

Table 3. LA-ICP-MS data on the bead composition in the area of the yellow decoration and base (wt %)

	yellow1	yellow2	yellow3	base1	base2	base3	base4	base5
B	<0.001	<0.001	<0.001	0.008	0.007	0.008	0.007	0.002
Na	0.173	0.142	0.187	0.051	0.045	0.041	0.088	0.119
Mg	0.020	0.006	0.013	0.024	0.020	0.017	0.025	0.027
Al	0.16	0.16	0.17	0.34	2.1	4.5	0.5	0.3
Si	9.9	9.1	10.7	17.0	17.6	17.4	16.6	16.2
P	0.1	<0.1	0.1	0.1	<0.1	<0.1	<0.1	0.3
K	0.09	0.04	0.15	9.2	10.7	11.3	9.2	8.3
Ti	0.03	0.03	0.02	0.06	0.06	0.05	0.06	0.06
Mn	0.003	0.004	0.011	0.99	0.75	0.46	0.99	0.99
Fe	0.095	0.031	0.050	0.17	0.16	0.19	0.16	0.20
Ni	0.003	0.004	0.003	<0.001	<0.001	<0.001	<0.001	<0.001
Cu	0.003	0.002	0.003	0.048	0.038	0.027	0.046	0.044
Zn	0.003	<0.001	0.002	0.009	0.008	0.006	0.009	0.010
Ga	<0.001	<0.001	<0.001	0.014	0.012	0.008	0.013	0.013
As	0.001	<0.001	0.001	0.001	<0.001	<0.001	0.001	0.001
Rb	<0.001	<0.001	<0.001	0.006	0.007	0.008	0.006	0.006
Sr	<0.001	<0.001	<0.001	0.003	0.002	0.002	0.003	0.005
Ag	0.002	0.002	0.002	<0.001	<0.001	<0.001	<0.001	<0.001
Sn	10.5	12.0	8.0	0.1	<0.001	<0.001	<0.001	<0.001
Sb	0.001	0.001	<0.001	<0.001	<0.001	<0.001	<0.001	<0.001
Ba	0.005	0.002	0.006	0.61	0.49	0.37	0.61	0.62
Pb	**61.1**	**61.5**	**61.9**	**45.4**	**40.3**	**36.3**	**46.2**	**47.8**

The content of elements Li, Be, V, Cr, Co, Sc, Ge, Y, Zr, Nb, Mo, Rh, Pd, Cd, In, Cs, La, Ce, Pr, Nd, Sm, Eu, Gd, Tb, Dy, Ho, Er, Tm, Yb, Lu, Hf, Ta, W, Re, Pt, Au, Tl, Bi, Th, U was less than 10^{-4} wt %.

color in this case was achieved due to a combination of factors. Unfortunately, we could not determine the glass color in a thin layer without destroying the object. On the one hand, the concentration of Fe along the lines of the white decor, determined by the method of large-scale XRF mapping, can be considered as con-tamination at the junctions of two glasses of different composition that have undergone severe corrosion. On the other hand, the fact that an increase in the Fe con-centration (Fig. 7e) on the SEM/EDS maps was detected in the region of the transverse section may indicate an attempt at additional decorative staining.

Tin oxide, which makes up 9.1−13.7% in the glass of the decoration, is an opacifier and dye of white color, and of yellow color in combination with lead.

Obviously, the base of the bead is made of glass of the K−Pb−Si class, and the decoration is made of glass of the Pb−Si class. The use of lead as a glass-forming element was noted in the Middle Ages in many regions of the Old World. As the main glass-forming element, lead stabilizes the glass and allows one to significantly reduce the melting temperature, thereby simplifying the process. In this role, lead has been known since antiquity ([42], p. 29) and very widely distributed. However, at the time of interest to us in the Golden Horde workshops in the Volga region, in Central Asia, glasses with a high lead content differed from the studied sample in a number of significant features: the presence of sodium, magnesium and manganese is noticeable in them. In a number of Central Asian glasses, potassium oxide can be detected in significant concentrations, but not exceeding 7.3%. At the same time, the vast majority of Asian glasses are distinguished by the variety and amount of impurities [43, 44].

Taking into account such features as minor impurities, the use of potash rather than ash, and the absence of specially introduced decolorizers, both identified classes are close to the Old Russian tradition of glass-making ([42], p. 19). However, a lower content of lead oxide in potash lead Old Russian glasses is noted: about 25−29% ([46], p. 654). O. Mecking, comparing them with those of European origin, distinguishes a special group of glasses produced in the workshops of Central Europe, on the territory of present Germany, the Czech Republic, Poland, and Slovakia. Glass containing on average 50.7% PbO, 37.8% SiO_2, and 11.5% K_2O was produced there, and the content of CaO is insignificant, similar to "Slavic" glasses, which is in good agreement with the glass composition of the studied bead ([46], pp. 654, 655). The workshop found by archaeologists in Erfurt worked until the very end of the 13th century. It is quite probable that

Table 4. LA-ICP-MS data on the composition of the yellow decoration and base material in oxides (%, averaged over all measurement points)

	Yellow	Base
Na_2O	0.224	0.093
MgO	0.021	0.038
Al_2O_3	0.308	2.95
SiO_2	21.200	36.6
K_2O	0.110	11.85
CaO		
TiO_2	0.043	0.099
MnO	0.008	1.090
Fe_2O_3	0.084	0.251
CuO	0.004	0.051
SnO	11.600	
PbO	66.400	47.000

Table 5. Results of XRF analysis

Mineral, %	Sample no.	
	1	2
Quartz (SiO_2)	50	16
Magnetite (Fe_3O_4)	11	23
Epidote ($Ca_2Al_2Fe^{3+}(SiO_4)_3OH$)	39	58
$PbSnO_3$		3

workshops could have functioned in this area also at a later time. We note that researchers of European compositions usually base their interpretations on the ratio of calcium and potassium oxides ([42], p. 84; [46]); calcium was not detected in the studied glass bead, although it was detected on its surface by the XRF method.

Fig. 8. Glass beads with superimposed decoration (*1*) and made of layered glass (*2*) from excavations of the Mininskii archaeological complex (according to ([32], Figs. 152, 153, 171)); (*3*) beads with "plastic" decoration (according to ([34], Fig. 15)); beads with "spiral-wavy" decoration and "superimposed threads" (nonspiral) of the Golden Horde period from (*4*) Bolgar, (*5*) Bilyar, and (*6*) Ukek (according to ([35], Figs. 82, 43, 44; [36], Figs. 29, 31, 32; [37], Figs. 1, 25−30, 34, 37, 38) respectively); (*7*) a bead from mound 6 of the Myakininskii archaeological complex (according to ([38], Fig. 166, *1a*)).

Volga-region beads of the Golden Horde period, according to the general opinion of experts, were made by applying glass threads to the body of the bead (for example, [41]). Also, according to the method of making the bead from Rostislavl, the Old Russian tradition with its characteristic individual spiraling and superimposed decoration is not confirmed and cases of making layered glass have not been recorded. The depth of white and yellow glass penetration up to 4 mm into the dark base (Fig. 6), established by X-ray tomography, excludes the imposition of glass strips from above with subsequent rolling (only the roller around one hole is superimposed on top). The manufacturing method is confirmed by a butt joint and inclusions of white and yellow glass inside the dark base, clearly visible on the polished area of the bead (Fig. 3). At the same time, it is impossible not to notice that the layered glass of the studied bead (as well as the indicated analogies in Fig. 8) differs from the manufacturing method of Middle Eastern glasses described by Francis, when layers of different colors alternated successively, then the resulting glass thickness was cut into even parts, connected in different directions, forming patterns of stripes and curved lines [20].

Layered glass beads similar to the studied specimen are described by L'vova from the earthen settlement of Staraya Ladoga. There, in the layers of the 10th century, there are specimens made, in her opinion, by the secondary treatment of multilayered glass by wrapping a sheet of glass around a hard rod, while the place of joining the glass sheet is clearly visible, as in our case ([47], p. 80). L'vova calls the Ladoga beads large ([47], Fig. 4, *4–6*), but does not indicate the exact dimensions; however, judging by the drawing, their diameter does not exceed 10 mm, they also differ in color from the Rostislavl specimen. Beads similar in manufacturing technique to the studied one are not known to us among European products.

Numerous small and large cavities inside the bead glass, apparently, correspond to gas inclusions; some of the pores could be formed as a result of damage to the glass. The latter circumstance can explain the presence of mineral inclusions; however, some of them should be uncooked components. A large number of gas inclusions indicates the use of glass that did not go through the clarification phase (which is in good agreement with mineral inclusions that did not enter into the reaction) ([48], pp. 23–25), or finished, reheated glass. With a high lead content, the temperature for softening the finished glass for the purpose of molding products was insignificant and was achieved even on an open fire. It is possible that glass, produced in another workshop, was used in its molding.

The unusually large weight of the studied object is given by a large amount of lead in its composition. Galibin indicates the maximum content of lead oxides in Old-Russian lead glasses up to 70% ([42], p. 82). Even more lead (85%) is contained in the glass com-

position of green and green-yellow transparent beads from the burials of the Old-Russian burial mound Myakinino in Moscow oblast ([49], p. 63, Table 6). Such a high content of this element is typical for small glass products: beads, pendants, bracelets. The studied bead is inferior in terms of the highest percentage of lead oxide to the maximum values known from publications of ~20%. At the same time, a high density of the object was established, indicating a significant content of this element in the glass. Possibly, the discrepancy is explained by the higher sensitivity of the chosen research methods compared with emission spectral analysis, which was used until recently for the vast majority of studied Old-Russian glasses.

It is interesting to note that when describing the corrosion of archaeological finds and the poor preservation of lead glasses, a crust on their surface is indicated ([31], p. 21). Experience shows that transparent lead glasses are chemically resistant, as can be seen from the example of Old-Russian bracelets. Opaque lead glasses with tin in the composition, in this case the decoration of the studied bead, are vulnerable to soil damage. A surface crust of indefinite color is typical of products made of potash-lead glasses, which we record on this bead. Studying and clarifying the relationship between the corrosion type of the glass and its chemical composition is extremely important: according to researchers, a visual analysis of the glass integrity allow one to draw conclusions about its origin ([50], p. 615), which is necessary when, for various reasons, accurate laboratory tests are unavailable.

CONCLUSIONS

As a result of studies of the morphology of the bead, its archaeological context and possible analogues, as well as the features of the elemental and phase composition in combination with visualization data, it can be concluded that the studied bead dates back to the 14th century. The performed tests allowed us to establish the composition and structure of the opaque glass and to clarify the methods of object manufacturing. The bead is made of layered glass of two classes: potash lead (dark base) and alkali-free lead (yellow and white decoration). A small amount of impurities, the absence of calcium oxide, and specially introduced decolorizers bring these glasses closer to the Old-Russian glass-making tradition, which does not correspond to the technique of object production: spiraling, individual and of small series, was used for Old-Russian beads. According to the percentage composition of the main glass-forming and the minimum presence of impurities, the dark glass of the base is closest to a special type of potash-lead glass from Central Europe. It should be noted that among the finds at medieval sites of Europe, the combination of different classes of glass in one object is known to researchers ([51], p. 587).

Judging from the internal structure, glass, which was not melted up to completion of the clarification

stage, was used for production of the object; mineral inclusions that did not enter the reaction remained in it, which is probably determined by the possibility of melting the glass with a significant content of lead at low temperatures.

The studied bead is unique for its time. An object with a similar glass composition was first identified on the territory of Old Russia. The layered structure of the glass was established exclusively due to precise nondestructive research methods. Beads with similar morphology (shape, color, size), are referred by archaeologists to beads with superimposed glass threads. In this case, the manufacturing technique turned out to be complex and not obvious in visual analysis. In combination with the chemical composition of the glass, we record here new handicraft traditions in Eastern Europe in the 14th century, which requires additional reflection in future research.

The unusual weight of the bead is due to the large amount of lead in the glass. Comparison with other lead glass objects is complicated by the use of different analytical methods. The difference in the lead percentage from the known maximum values can be explained by the use of more sensitive methods of analysis in this work. The further accumulation of information on the composition of Old-Russian glasses using the latest analytical research methods should clarify the situation with the maximum values of lead oxides and other glass-forming elements, showing a huge scatter today.

For the conducted study, it is important that the studied object characterizes the material culture of the population of the 14th century. This is a time of global changes in the Russian lands: due to a whole range of causes, the status of many settlements and the structure of rural settlement are changing, significant changes are taking place in the social sphere, noticeable changes in material culture [52]. Despite the success of intensive archaeological studies in recent decades, many features of the material culture of that time still remain unclear. Therefore, new information about the traditions of working with glass in that period is extremely important for a deeper understanding of the processes that took place in that period.

CONFLICT OF INTEREST

We declare that we have no conflict of interest.

REFERENCES

1. N. A. Makarov, I. E. Zaitseva, and E. A. Greshnikov, Arkheol. Vesti, No. 23, 291 (2017).
2. N. N. Kolobylina, E. A. Greshnikov, A. L. Vasiliev, E. Yu. Tereschenko, I. E. Zaytseva, N. A. Makarov, P. K. Kashkarov, E. B. Yatsishina, and M. V. Koval-chuk, Crystallogr. Rep. **62**, 529 (2017).
3. N. A. Makarov, E. A. Greshnikov, I. E. Zaitseva, et al., Kratk. Soobshch. Inst. Arkheol., No. 258, 25 (2020).
4. L. I. Govor, E. A. Greshnikov, I. E. Zaitseva, et al., Kratk. Soobshch. Inst. Arkheol., No. 249-II, 348 (2017).
5. E. S. Kovalenko, K. M. Podurets, E. A. Greshnikov, I. Y. Zaytseva, S. S. Agafonov, V. A. Somenkov, N. N. Kolobylina, A. A. Kaloyan, L. I. Govor, V. A. Kurkin, and Y. B. Yatsishina, Crystallogr. Rep. **64**, 841 (2019).
6. I. E. Zaitseva, E. A. Greshnikov, A. A. Veligzhanin, et al., Ross. Arkheol., No. 3, 50 (2019).
7. E. A. Greshnikov, V. M. Pozhidaev, S. N. Malakhov, et al., Ross. Arkheol., No. 4, 165 (2020).
8. A. Yu. Loboda, A. V. Mandrykina, I. E. Zaitseva, E. Yu. Tereschenko, and E. B. Yatsishina, Nanotechnol. Russ. **16**, 607 (2021).
9. A. Yu. Loboda, A. V. Mandrykina, I. E. Zaitseva, et al., Nanotechnol. Russ. **17** (5), 655 (2022).
10. E. K. Stolyarova, E. S. Kovalenko, M. M. Murashev, et al., *Medieval Arts and Crafts. To the 90th Anniversary of the Birth of T. I. Makarova* (IA RAN, Moscow, 2021), p. 18 [in Russian].
11. S. I. Valiulina, O. S. Rumyantseva, E. S. Vashchenkova, et al., Ross. Arkheol. No. 3, 107 (2022).
12. M. V. Kovalchuk, N. A. Makarov, E. B. Yatsishina, A. A. Antsiferova, P. V. Dorovatovskii, E. A. Greshnikov, P. K. Kashkarov, S. N. Malakhov, S. V. Olkhovskii, N. N. Presniakova, and R. D. Svetogorov, Crystallogr. Rep. **64**, 1003 (2019).
13. M. V. Kovalchuk, E. B. Yatsishina, N. A. Makarov, E. A. Greshnikov, A. A. Antsiferova, O. L. Gunchina,

P. K. Kashkarov, E. S. Kovalenko, M. M. Murashev, S. V. Olkhovskii, K. M. Podurets, and V. B. Timerkaev, Crystallogr. Rep. **65**, 805 (2020).

14. P. K. Kashkarov, M. V. Kovalchuk, N. A. Makarov, E. B. Yatsishina, E. A. Greshnikov, A. A. Antsiferova, P. A. Volkov, L. I. Govor, S. V. Olkhovsky, N. N. Presniakova, and R. D. Svetogorov, Crystallogr. Rep. **66**, 165 (2021).

15. A. S. Pakhunov, E. G. Devlet, I. A. Karateev, R. D. Svetogorov, P. V. Dorovatovskii, R. A. Senin, A. E. Blagov, and E. B. Yatsishina, Crystallogr. Rep. **63**, 1027 (2018).

16. V. Yu. Koval', in *Archeology of the Moscow Oblast, Proceedings of the Scientific Seminar,* Ed. by A. V. Engovatov (IA RAN, Moscow, 2004), p. 8.

17. V. Yu. Koval', in *Archeology of the Moscow Oblast, Proceedings of the Scientific Seminar*, Ed. by A. V. Engovatov (IA RAN, Moscow, 2017), No. 13, p. 99.

18. V. Yu. Koval', Report on Archaeological Excavations at the Settlement of Rostislavl and the Settlement of Sosnovka IV in the Ozersky District of the Moscow Oblast in 2018−2019, *Archive of IA RAS,* R-1 (2020).

19. A. V. Artsikhovskii, *Vyatichi Burial Mounds* (RANI ON, Moscow, 1930) [in Russian].

20. P. Francis, Jr., Beads, No. 1, 21 (1989).

21. A. A. Abdurazakov, M. A. Bezborodov, and Yu. A. Zadneprovskii, *Glassmaking in Central Asia in Antiquity and the Middle Ages* (Akad. Nauk Uzbek. SSR, Tashkent, 1963) [in Russian].

22. C. A. Schneider, W. S. Rasband, and K. W. Eliceiri, Nat. Methods **9**, 671 (2012).
https://doi.org/10.1038/nmeth.2089

23. G. T. Herman, *Fundamentals of Computerized Tomography: Image Reconstruction from Projections* (Academic, New York, 1980).

24. M. Dierick, B. Masschaele, and L. van Hoorebeke, Meas. Sci. Technol. **15**, 1366 (2004).
https://doi.org/10.1088/0957-0233/15/7/020

25. www.volumegraphics.com/en/products/vgstudio/what-s-new-in-vgstudio-3-5-x.

26. T. A. Karimova and G. L. Bukhbinder, Zavod. Labor. Diagn. Mater. **85** (6), 24 (2019).

27. O. S. Rumyantseva, A. A. Trifonov, and D. A. Khanin, *Bryansk Treasure of Jewellery with Chiseled Enamel of the Eeastern European Style (3D Century AD)* (IA RAN, Drevnosti Severa, Vologda, 2018), p. 199 [in Russian].

28. R. D. Svetogorov, P. V. Dorovatovskii, and V. A. Lazarenko, Cryst. Res. Technol. **55**, 1900184 (2020).

29. R. D. Svetogorov, "Dionis - Diffraction Open Integration Software," State Registration Certificate of Computer Program No. 2018660965.

30. C. R. Hubbard, E. H. Evans, and D. K. Smith, J. Appl. Crystallogr. **9**, 169 (1976).

31. A. K. Elkina, N. L. Podvigina, I. A. Khazanova, et al., *Field Conservation of Archaeological Finds (Textiles, Metal, Glass), Guidelines* (Moscow, 1987) [in Russian].

32. S. D. Zakharov and I. N. Kuzina, *Archeology of the Northern Russian Village of the 10th−13th Centuries: Medieval Settlements and Burial Grounds on Lake Kubenskoe,* Ed. by N. A. Makarov, Vol. 2: *Material Culture and Chronology,* Ed. by S. D. Zakharov (Nauka, 2008), p. 142 [in Russian].

33. S. D. Zakharov, *The Ancient Russian City of Beloozero* (Indrik, 2004) [in Russian].

34. Yu. L. Shchapova, *Glass of Kievan Rus* (Mosk. Gos. Univ., Moscow, 1972) [in Russian].

35. S. I. Valiulina and L. F. Nedashkovskii, Nizhnevolzh. Arkheol. Vestn., No. 7, 257 (2005).

36. M. D. Poluboyarinova, *City of Bolgar. Essays on Handicraft Activities* (Nauka, Moscow, 1988), p. 151 [in Russian].

37. S. I. Valiulina, *Glass of the Volga Bulgaria (According to the Materials of the Bilyar Settlement)* (Kazan. Univ., Kazan', 2005) [in Russian].

38. A. V. Engovatova, V. Yu. Koval', E. P. Zots, et al., *Myakinin Mounds. Myakininsky Archaeological Complex in the Moscow Oblast,* Vol. 21 of *Materials of Rescue Archaeological Research* (IA RAN, Moscow, 2018) [in Russian].

39. J. Callmer, *Trade Beads and Bead Trade in Scandinavia ca. 800–1000 A. D.* (Bonn, Lund, 1977).

40. M. Markiewicz, *Biżuteria szklana z wczesnośredniowiecznych cmentarzysk strefy chełmiǹsko-dobrzyǹskiej (część północno zachdnia),* Vol. 4 of *Series Mons Sancti Laurentii* (Uniw. Mikołaja Kopernika, IA RAN, Toruń, 2008).

41. L. L. Galkin, Sov. Arkheol., No. 2, 213 (1984).

42. V. A. Galibin, *Glass Composition as an Archaeological Source,* Vol. 11 of *Archaeologica Petropolitana* (Peterb. Vostokoved., St. Petersburg, 2001) [in Russian].

43. S. I. Valiulina, in *Pax Mongolica and Eurasian Shocks in the 13th–14th Centuries,* Stratum plus, No. 6, 337 (2016).

44. S. Valiulina, in *Proceedings of the 39th International Symposium for Archaeometry, Leuven, May 28–June 1, 2012,* Ed. P. Degryse (Leuven, 2014), p. 280.

45. S. I. Valiulina, Uch. Zap. Kazan. Univ., Guman. Nauki **10** (1), 14 (2008).

46. O. Mecking, Archaeometry **55**, 640 (2013).

47. Z. A. L'vova, in *Archaeological Collection of the State Hermitage* (Gos. Ermitazh, Leningrad, 1968), No. 10, p. 64 [in Russian].

48. N. Kachalov, *Glass* (Akad. Nauk SSSR, Moscow, 1959) [in Russian].

49. E. K. Stolyarova, *Myakinin Mounds. Myakininsky Archaeological Complex in the Moscow Oblast,* Vol. 21 of *Materials of Rescue Archaeological Research* (IA RAN, Moscow, 2018), p. 60 [in Russian].

50. I. C. Freestone, in *Handbook of Archaeological Sciences,* Ed. by D. R. Brothwell and A. M. Pollard (Wiley, New York, 2001), p. 615.

51. A. Pankiewicz and S. Siemianowska, Archeol. Rozhledy **72**, 573 (2020).

52. N. A. Makarov, in *Rus in the XIII Century: Antiquities of the Dark Age,* Ed. by N. A. Makarov and A. V. Chernetsov (Nauka, Moscow, 2003), p. 5 [in Russian].

Translated by D. Novikova